

# DISK DISPERSAL AROUND YOUNG STARS

DAVID HOLLENBACH

*NASA-Ames Research Center, Moffett Field, CA*

HAROLD W. YORKE

*Jet Propulsion Laboratory, California Institute of Technology, Pasadena, CA*

and

DOUG JOHNSTONE

*Canadian Institute for Theoretical Astrophysics, Toronto*

We review the evidence pertaining to the lifetimes of planet-forming disks and discuss possible disk dispersal mechanisms: 1) viscous accretion of material onto the central source, 2) close stellar encounters, 3) stellar winds, and 4) photoevaporation by ultraviolet radiation. We focus on 3) and 4) and describe the quasi-steady state appearance and the overall evolution of disks under the influence of winds and radiation from the central star and of radiation from external OB stars. Viscous accretion likely dominates disk dispersal in the inner disk ( $r \lesssim 10$  AU), while photoevaporation is the principal process of disk dispersal outside of  $r \gtrsim 10$  AU. Disk dispersal timescales are compared and discussed in relation to theoretical estimates for ~~planet formation~~ <sup>planet</sup> timescales. Photoevaporation may explain the large differences in the hydrogen content of the giant planets in the solar system. The commonly held belief that our early sun's stellar wind dispersed the solar nebula is called into question.

*ISM*  
*circumstellar disks*    *circumstellar matter*  
*protoplanetary disks*    *H II regions*  
*star formation*    *planet formation*

## I. INTRODUCTION

The question of planet formation is intimately related to the formation and evolution of disks around condensing protostars. When considering the evolution of dust grains through the planetesimal stage up to the creation of (proto-)planets, it is important to realize that the disks themselves are continually evolving. Indeed, very short-lived disks may not have sufficient time to produce planets.

In the standard theory of low mass star formation and disk evolution, a rotating, collapsing molecular core accretes at a rate  $\dot{M}_c \sim 10^{-6} - 10^{-5} M_\odot \text{ yr}^{-1}$ , initially directly onto the protostar, but soon mainly onto an orbiting accretion disk around the protostar (Terebey, Shu, & Cassen 1984). This rapid accretion quickly builds up the disk

mass  $M_d$  until gravitational instabilities set in, when the disk mass is roughly  $\sim 0.3M_*$ , where  $M_*$  is the mass of the protostar (Laughlin & Bodenheimer 1994; Yorke, Bodenheimer, & Laughlin 1995). The gravitational instabilities produce spiral density waves, which allow angular momentum to be transported outwards. The disk material can then be transferred onto the protostar at nearly the same rate as the disk accretes material from the molecular core; the disk “hovers” at the critical gravitationally unstable limit,  $M_d \sim 0.3M_*$ , as the star grows. The result at the end of the accretion phase could be, for example, a  $1 M_\odot$  star with a  $\sim 0.3 M_\odot$  disk.

Once the cloud stops accreting onto the disk, the epoch of disk and stellar growth ceases. As the disk mass falls below the level required for gravitational instability, the transfer of angular momentum drops considerably and other, less efficient processes for transport take over, possibly turbulent or magnetic (Balbus & Hawley 1991). This phase might be identified with the class II, or T Tauri phase of disk evolution, and observations of the excess blue emission from the accretion of the disk onto the star suggest median mass accretion rates of order  $10^{-8} M_\odot \text{ yr}^{-1}$  with an order of magnitude scatter (Hartmann et al. 1998). As the disk loses mass, this rate should decrease. Whether the lifetime of the disk is thereafter determined by the evolution of the viscosity in the disk, which controls the accretion rate onto the star, or whether other processes such as winds and ultraviolet radiation eventually dominate disk dispersal is part of the subject of this paper.

Observational estimates of disk masses around young pre-main-sequence stars typically give values that are less than 10% the mass of the central star (Adams, Emerson, & Fuller 1990; Beckwith et al 1990); often a value closer to 1% can be inferred. An example of a well-determined and relatively high-mass disk is that of GM Aurigae (Koerner, Sargent, & Beckwith 1993), a star of  $0.72 M_\odot$  with a disk of  $0.09 M_\odot$ . In spite of some uncertainty in the mass estimates, these values for the later stages of disk evolution are in contrast to the  $\sim 0.3M_*$  discussed above for disks still accreting material from the parent cloud. This implies non-negligible disk evolution after accretion stops.

The *dust* in the inner disks around low mass stars apparently disappears in about  $10^7$  years, whereas disks around intermediate mass stars appear to be depleted in somewhat shorter timescales (Strom 1995). Using pre-main sequence evolutionary models to calculate the ages of star-forming clusters, and counting the numbers of stars found with and without observable inner disks, Strom showed that for very young ( $\sim 10^6$  yr old) clusters such as Ophiuchus, almost all pre-main sequence stars have disks, whereas for older regions the fraction of stars with disks drops as the mass of the star in question rises. A small fraction, perhaps 10%, of low-mass stars still have disks beyond 10 Myr. Therefore, the (inner) disk dispersal timescale for low mass

( $M_* \lesssim 3 M_\odot$ ) stars may be of order  $\tau_d \sim 10^7$  years.

These constraints on the evolution of the disk can be compared to the formation of giant planets in the solar system. Current theoretical thinking envisages a typical giant planet in the outer solar system to form by (1) the accumulation of solid (comet-like) planetesimals to ever larger bodies (Safronov 1969, Wetherill 1980, Nakagawa et al. 1983) (timescale  $\lesssim 10^5$  years, Weidenschilling 1984), until (2) a runaway growth occurs for the largest planetary embryos (Greenberg et al. 1978, 1984), with the runaway halted only after the depletion of the planetesimals in a given embryo's "feeding zone" and the embryos become gravitationally isolated from one another (at a mass  $\sim 1 M_\oplus$  in the giant planet region for a "minimum" solar nebula); followed by (3) a much slower agglomeration of individual embryos into the core of each of the current planets (Wetherill & Stewart 1986), until (4) the core reaches a critical mass ( $\sim 15 - 20 M_\oplus$ ) and begins to gather in gas much faster than it gathers solids (Mizuno 1980, Bodenheimer & Pollack 1986, Pollack et al. 1996), followed yet later by (5) the cessation of gas and solid accretion when tidal forces inside the Hill sphere suffice to open up a gap around the planet (Papaloizou & Lin 1984; Lin & Papaloizou 1985, 1986a,b). Protostellar disks can therefore be partially destroyed by the transformation of the gas and dust into planets.

However, it is clear that considerably more mass was dispersed by other mechanisms than was congealed into planets. If the solar nebula had only the "minimum mass" needed to form the known planets ( $\sim 0.013 M_\odot$  according to Hayashi et al. 1985), the timescale needed to assemble the giant planets ranges from  $\sim 10^8$  yr for Jupiter to  $\sim 10^{11}$  yr for Neptune (Nakagawa et al. 1983), much too long to explain many observed features of the solar system (such as the existence of the asteroid belt and of Neptune). Lissauer (1987, 1993) has proposed that the timescale problem can be alleviated by postulating a solar nebula that contained much more mass than the "minimum" value. Increases by a factor of 5-10 in the giant-planet zones would push the embryo isolation-mass to or beyond the critical core mass, which would eliminate the slow process (3) of accumulation, allowing Jupiter, Saturn, Uranus, and Neptune to form on timescales of  $\sim 10^6$ - $10^8$  yr. The core growth occurs then on timescales of  $\sim 3 \times 10^6 (r/10AU)^{3/2}$  yr and the gas accretion onto the cores at times  $\gtrsim 10^6 - 10^7$  yr. Even if the solar nebula originated with only the minimum mass, there is clear evidence for disk dispersal by mechanisms other than planet formation. In accounting for the elemental abundances in the solar planets, one finds that the hydrogen and helium are deficient by a large factor compared to the original cosmic abundances which formed the planets. Clearly, the early solar nebula incorporated many of the heavier elements in the terrestrial planets and rocky cores, but substantial hydrogen and helium-rich gas was dispersed by other mechanisms. In addition, we

note that the recent detections of extrasolar planets give no indication that a high fraction of the  $\sim 0.01 M_{\odot}$  disks observed around young low mass stars has been transformed entirely into planets. Therefore, we conclude that planet formation is a minor disk dispersal mechanism. This paper focuses instead on the dispersal timescales of other mechanisms in order to understand the time available for the above processes of planet formation to operate.

A number of mechanisms, both internal and external, disperse the gas and dust disks around young stars or protostars. These processes can be so efficient that the disks may not have sufficient time to form planets, or the planets formed may be dispersed with the nebular material. For example, viscosity in the disk (see §IIA) coupled with the tidal force of a relatively massive disk on embedded giant planets may result in inwardly migrating planets which can be accreted, along with gas and dust, onto the central star (Lin, Bodenheimer, & Richardson 1996). Close encounters with binary or cluster companions can strip and truncate the outer disks, and can liberate the outer planets (§IIB). Stellar winds have often been postulated as a likely mechanism to entrain and push the gas and dust in the disk and to drive it into the interstellar medium (§IIC). The ultraviolet radiation from the central star or an external star can heat the outer disks and cause them to evaporate on relatively short timescales (§IID). Obviously, understanding disk dispersal timescales is crucial to predicting the final product of planetary formation.

## II. DISK DISPERSAL MECHANISMS

In our discussion of disk dispersal mechanisms, we shall focus on the dispersal of disk material at distances  $\gtrsim 1$  AU from the central star, where terrestrial and giant planets may form and where the bulk of the mass of the young disk presumably resides, assuming a surface density distribution  $\Sigma \propto r^{-\beta}$  with  $\beta < 2$ . We also focus on the early stages of disk evolution and the dispersal of the bulk of the original disk, rather than the later stages of dispersal of remnant disks, such as the one around  $\beta$  Pic. There are four basic processes for disk dispersal other than planet formation: (A) accretion of disk material onto the central source, (B) stripping due to close stellar encounters, (C) the removal of disk material due to the effects of stellar or disk winds, and (D) photoevaporation due to the ultraviolet radiation from the central source and/or close companions. All of these interactions operate concurrently and we will discuss how winds can enhance photoevaporation. Considerable progress has been made since the last Protostars and Planets meeting in understanding the last of these mechanisms, so we devote a large proportion of our review to photoevaporation.

### A. Disk Accretion

Radial mass flow in disks is a well studied, although still not completely understood, phenomenon. The transport of angular momentum outward allows disk material to radially flow inward. The angular momentum can be transported, for example, by turbulence or magnetic fields, and often the physics of the evolution is subsumed in a parameter  $\alpha$  which fixes the effective viscosity which drives radial accretion through the disk.

Parameterizing the viscosity by  $\nu = \alpha c_S H$  (Shakura & Sunyaev 1973, Pringle & Rees 1972), where scale height  $H$  and sound speed  $c_S$  are given by  $H = r c_S / (GM_*/r)^{1/2}$  and  $c_S = (kT/m_H)^{1/2}$ , we find  $\nu \propto r$ , if the temperature in the disk follows a  $T \propto r^{-1/2}$  power law. Given that the viscous timescale  $t_\nu \simeq r^2/\nu$ , it follows  $t_\nu \propto r$ :

$$t_\nu \simeq 10^5 \text{ yr} \left( \frac{\alpha}{0.01} \right)^{-1} \left( \frac{r}{10 \text{ AU}} \right)$$

The viscous dispersal timescale is plotted in Fig. 1 for two values of  $\alpha$  ( $10^{-3}$  and  $10^{-2}$ ) thought to best represent the effective viscosity in protoplanetary disks (see, e.g., Hartmann et al. 1998). Assuming disk angular momentum is constant and that  $\beta < 2$  so that the disk mass resides mostly at the outer disk radius  $r_d$ , it follows that  $r_d(t) \propto M_d(t)^{-2}$ . Therefore, as the disk accretes matter onto the central star, it preserves its angular momentum by expanding to greater size. For times greater than the initial timescale  $t_{\nu 0}$

$$r_d \simeq r_{d0} \left( \frac{t}{t_{\nu 0}} \right) \quad \text{and} \quad M_d(t) \simeq M_{d0} \left( \frac{t}{t_{\nu 0}} \right)^{-1/2},$$

where  $r_{d0}$  and  $M_{d0}$  are the initial radius and mass of the disk at  $t_{\nu 0}$ . As the disk grows, the viscous timescale in the outer regions, where the mass resides, gets longer. Therefore, viscous accretion may account for the dispersal of the inner parts of disks, but become insignificant for the outer disks and cannot explain the complete dispersion of the disk.

For  $M_{d0} = 0.1 M_\odot$  the mass accretion rate onto the central star, or the accretion mass loss rate from the disk, is given for  $t > t_{\nu 0}$

$$\dot{M}_\nu \simeq 5 \times 10^{-7} M_\odot \text{ yr}^{-1} \left( \frac{\alpha}{0.01} \right) \left( \frac{r_{d0}}{10 \text{ AU}} \right)^{-1} \left( \frac{t}{t_{\nu 0}} \right)^{-3/2}$$

### B. Stellar Encounters

The effects of close stellar encounters on protostellar disks have been discussed by Clarke & Pringle (1993), Heller (1995), Hall et al (1996),

Larwood (1997) and Bonnell & Kroupa (1998). Typically, the disk (and any outer planets) is stripped to about 1/3 the impact parameter  $r_p$  in a single close encounter. From this we can estimate the timescale  $t_{SE}$  to truncate a disk to the radius  $r_d$ :  $t_{SE} \simeq 1/n_*\sigma v$ , where  $n_*$  is the density of stars,  $\sigma \simeq \pi(3r_d)^2$  is the collision cross section and  $v$  is the velocity dispersion of stars:

$$t_{SE} \simeq 2 \times 10^7 \text{ yr} \left( \frac{n_*}{10^4 \text{ pc}^{-3}} \right)^{-1} \left( \frac{v}{1 \text{ km s}^{-1}} \right)^{-1} \left( \frac{r_d}{100 \text{ AU}} \right)^{-2}.$$

This timescale is also shown in Fig. 1.

### C. Effects of Winds on Disks

Although protostellar winds and outflows were a great surprise when first observed some two decades ago, we are now beginning to understand the origin of the winds and the wind environment in the vicinity of circumstellar disks. During and after the cloud collapse phase which builds up the disk mass, the disk actively accretes onto the protostar ( $t \lesssim 10^7$  yr) and creates a strong wind. The interaction of the rotating magnetic field with the inner disk produces this wind whose mass loss rate ( $\dot{M}_w \sim 10^{-7} M_\odot \text{ yr}^{-1}$  [for  $t \sim 10^6$  yr] –  $10^{-8} M_\odot \text{ yr}^{-1}$  [for  $t \sim 10^7$  yr]) is about 0.3–0.5 times the accretion rate onto the protostar (Shu et al 1988, Königl 1995, Ouyed & Pudritz 1997a,b). The terminal wind speeds are of order 100–200 km s<sup>-1</sup>. The mass lost in these strong winds is disk material ejected via coupling between the (weakly) ionized disk gas and the outward bending magnetic field. These disk winds are not spherically symmetric, but are magnetically collimated away from the disk plane towards the poles. Later, as the accretion subsides, the magnetic activity in the chromosphere of the young, low mass star drives a (spherically symmetric) stellar wind, which is likely much more active in the early ( $\sim 10^7$  yr) epoch than the current solar wind ( $\dot{M}_w \sim 10^{-13} M_\odot \text{ yr}^{-1}$ ).

As an upper limit to the dispersing power of disk winds, we will ignore their collimation and consider the momentum transferred by the collision of spherically symmetric winds with the disk (c.f. Fig. 2). The scale height of cold ( $c_S \sim 0.1 (GM_*/r)^{1/2}$ ), protostellar disks is of order  $H \sim 0.1r$ , which implies that the fraction of solid angle subtended by cold disks is of order 0.1. Assuming that stripping occurs in a thin mixing layer at a height  $z_s(r)$  above the disk and that disk gas can flow into this mixing region at a maximum velocity of  $\epsilon c_S$ , where  $\epsilon \simeq 0.01 - 0.1$  (Canto & Raga 1991), the mass loss rate can be approximated by  $\dot{M}_{ws} = 2 \int_{r_*}^{r_d} \epsilon \rho(r, z_s) c_S(r) 2\pi r dr$ . In the thin mixing layer at  $z_s(r)$ , the normal component of the wind ram pressure  $(\sin \theta)^2 (\dot{M}_w v_w / 4\pi r^2)$  equals the disk gas pressure  $\rho(r, z_s) c_S^2(r)$ , where  $\theta$  is the angle between the incident wind and the wind shock which

traces the top of the mixing layer. Substituting this relation into the mass loss equation and assuming that  $c_S(r)$  declines with  $r$ , we conclude that the maximum mass loss rate  $\dot{M}_{ws}$  and the minimum dispersal timescale  $t_{ws}$  from wind stripping are given by

$$\dot{M}_{ws} \simeq 4 \times 10^{-2} \dot{M}_w \left( \frac{v_w}{100 \text{ km s}^{-1}} \right) \left( \frac{\overline{\epsilon(\sin \theta)^2}}{10^{-4}} \right) \left( \frac{T(r_d)}{100 \text{ K}} \right)^{-1/2}$$

and

$$t_{ws} \simeq 10^7 \text{ yr} \left( \frac{r}{1 \text{ AU}} \right)^{1/4} \left( \frac{\overline{\epsilon(\sin \theta)^2}}{10^{-4}} \right)^{-1} \left( \frac{M_d}{M_{\min}} \right) v_{w7}^{-1} \dot{M}_{w-8}^{-1} ,$$

where  $v_{w7} = v_w/100 \text{ km s}^{-1}$ ,  $\dot{M}_{w-8} = \dot{M}_w/10^{-8} M_\odot \text{ yr}^{-1}$ ,  $\overline{(\sin \theta)^2}$  is the integral-averaged value of  $(\sin \theta)^2$ , and  $M_{\min} \simeq 0.01 M_\odot$  is the minimum mass solar nebula. We have numerically computed  $\overline{(\sin \theta)^2} \sim 10^{-3}$  for a reference model with  $\dot{M}_{w-8} = 1$ ,  $v_{w7} = 1$ , and  $M_d = M_{\min}$ .

Stellar wind dispersal has been postulated as a mechanism for the dispersal of stellar disks (Cameron 1973, Horedt 1978, 1982 and Elmegreen 1979). However, as can be seen in Fig. 1 where various disk dispersal timescales are compared to one another, wind stripping should not be an effective disk dispersal mechanism for a reasonably flat (cold) disk, assuming  $\overline{\epsilon(\sin \theta)^2} \lesssim 10^{-4}$ .

Two separate arguments support this conclusion. First, Richling & Yorke (1997) have done numerical simulations which include the ultraviolet-induced photoevaporation of the disk (see §D below) acting simultaneously with (isotropic) wind stripping. The ultraviolet-heated disk atmosphere and photoevaporative flow deflects and collimates the wind, and reduces the wind stripping significantly. A low degree of mixing between the winds and the disk outflows is found. Although no numerical simulations exist for the particular configuration of interacting T Tauri disks and winds, one can infer from the results of Richling & Yorke that the value for  $\overline{\epsilon(\sin \theta)^2}$  is indeed low. Secondly, we note that the strong protostellar (disk) winds collimate quickly, probably by magnetic forces, and for this reason alone are unlikely to aid in the removal of material from the outer disk (see for example recent HST images of DG Tau (Kepner et al 1993) and HH30 (Stapelheldt et al 1994; Burrows et al 1996)).

Further work should be done to test for instabilities which could significantly raise  $\epsilon$  and to exhaustively study the parameter space of disk properties to test the variations in  $(\sin \theta)^2$ . In the absence of these results, the wind dispersal timescales plotted on Fig. 1 ( $t_{ws} \equiv \Sigma(r)/\dot{\Sigma}(r)$ , where  $\Sigma(r)$  is the surface density at  $r$ ) are only improved versions of previous work, but still uncertain by perhaps an order of magnitude. Nevertheless, we suggest that wind stripping is probably not as significant as viscous accretion and photoevaporation.

## D. Photoevaporation

Disk photoevaporation was first proposed for high-mass stars with disks because these stars have extremely powerful Lyman continuum fluxes. One of the main motivations was to explain the relative long lifetimes of small ( $r \lesssim 10^{17}$  cm) and dense ( $n_e \gtrsim 10^4 - 10^5$  cm $^{-3}$ ) ultracompact HII (UCHII) regions. The high densities and temperatures of these regions compared to molecular clouds as a whole suggest that UCHII regions are overpressurized and should expand at velocities in excess of  $c_S \sim 10$  km s $^{-1}$ . Without replenishment of this gas, the dynamical timescale of  $\sim 10^{3.5}$  yr predicts that these regions should quickly expand and become more diffuse. However, Wood & Churchwell (1989) performed a radio survey of UCHII regions, and found that 10-20% of all O stars are in the UCHII phase. Given that O stars live approximately  $10^{6-7}$  yr, this implies that dense UCHII regions last for  $10^{5.5}$  yr, two orders of magnitude longer than the dynamical timescale.

Whereas the idea of using the photoevaporation process as a means for eroding disks around young massive stars had been mentioned occasionally in the literature (e.g., Bally & Scoville 1982), Hollenbach et al (1993, 1994, hereafter HJLS94) first applied the idea rigorously as a model for ultracompact HII regions. The first numerical studies of this process (Yorke & Welz 1993, 1994) have been supplemented by more realistic simulations including the effects of UV dust scattering (Richling & Yorke 1997) and photoevaporating the disks of close companions in a multiple system (Richling & Yorke 1998a, 1998b). HJLS94 proposed that UCHII regions live for  $10^{5.5}$  yr because they are constantly being replenished by a dense circumstellar reservoir — the orbiting disk. Although the high-pressure gas expands away from the disk at speeds of 10–50 km s $^{-1}$ , the disk reservoir maintains a quasi-steady state density and intensity profile. The photoevaporating disk model matches well with the morphology, emission measure and spectrum of a number of UCHII regions. As we shall demonstrate in the following, the mass loss rate  $\dot{M}_{ph}$  from the disk around an O star with a Lyman continuum photon luminosity  $\Phi_i \sim 10^{49}$  s $^{-1}$  is of order a few times  $10^{-5} M_\odot$  yr $^{-1}$ . Therefore, if massive O stars are born with disks with mass  $\sim 0.1 - 0.3 M_*$ , the timescale to photoevaporate the disk is  $10^{5.5}$  years. Although this timescale is long enough to explain UCHII regions, it is sufficiently short to significantly impact the formation of planets around high mass stars.

Surface disk material efficiently evaporates when it is heated to temperatures such that the average thermal speeds of the atoms or ions are comparable to the escape speed from the gravitational potential. Photoionization of hydrogen by Lyman continuum (EUV,  $h\nu > 13.6$  eV) photons heats the gas at the surface of the disk to temperatures  $T \sim 10^4$  K forming an ionized atmosphere or corona above the

disk. Beyond a critical distance from the central star,  $r_g \simeq GM_*/c_S^2$  ( $\sim 10^{14} [M_*/M_\odot]$  cm), the heated gas becomes unbound and produces a thermal disk wind. Massive stars radiate copious EUV photons which rapidly photoevaporate their outer disks. Young low mass stars also have sufficient Lyman continuum flux to photoionize their outer disk material and create an appreciable photoevaporative flow. Alternatively, nearby massive stars in star-forming regions produce large fluxes of both EUV and FUV ( $6 \text{ eV} < h\nu < 13.6 \text{ eV}$ ) photons which can heat and evaporate the circumstellar disks around young low-mass stars.

### 1. Photoevaporation by the central star: physical processes and semi-analytical models

The ultraviolet flux from the central star can be divided into the Extreme Ultraviolet (EUV, capable of ionizing hydrogen) and the Far Ultraviolet (FUV, capable of dissociating  $\text{H}_2$  and CO and ionizing C). The EUV flux ionizes and heats the surface of the disk to  $10^4$  K. The FUV flux penetrates the HII region created by the EUV flux, and heats a primarily neutral layer of H and  $\text{H}_2$  to temperatures of order 100–3000 K, depending on the magnitude of the flux and the density of the gas. These regions in the interstellar medium are often called Photodissociation Regions, or PDRs (e.g. Hollenbach & Tielens 1997).

Previous work has treated the effect of EUV photons, and we shall focus on that case here. However, the FUV photoevaporation by the central star is nearly completely analogous, and we will remark on the small differences for this case as they arise. We will also normalize our equations for the case of the photoevaporation by a low mass ( $M_* = 1M_\odot$ ) star, with an estimated EUV photon luminosity of  $10^{41} \text{ s}^{-1}$ . However, the equations are equally applicable to high mass stars (indeed, as noted above, they were originally derived for this case).

*Weak Stellar Wind Case.* If the central star has a “weak” stellar wind (we shall quantitatively describe the criterion for a weak wind below), then photoionization of the neutral hydrogen on the surface of the inner region of the disk should result in the formation of a bound ionized atmosphere with  $T \sim 10^4$  K (c.f. Fig. 3a). Inside  $r_g \simeq 10 \text{ AU } M_*/M_\odot$ , where the sound velocity is less than the escape velocity, the atmosphere can be approximated as hydrostatic and isothermal. The density of ionized hydrogen  $n(r, z)$  in the inner region depends on the density at the base of the HII atmosphere  $n_0(r)$  and the height  $z$  above the disk according to  $n(r, z) = n_0(r) \exp(-z^2/H^2)$ , where the scale height is given by:  $H(r) = r^{3/2}/r_g^{1/2}$  (HJLS94). Note that  $H(r_g) = r_g$ .

Outside of  $r_g$  the evaporated material flows from the disk at approximately the sound speed  $v \sim c_S \simeq 10 \text{ km s}^{-1}$ . Here,  $n(r, z) \simeq n_0(r)$  yields a reliable estimate near the disk ( $z < r$ ), where the flow has little opportunity to expand. The mass loss rate from the disk  $\dot{M}_{ph}$  is given

by  $\dot{M}_{ph} = 2m_{HCS} \int_{r_g}^{\infty} 2\pi n_0(r) r dr$ , where the first factor of 2 accounts for both faces of the disk and  $m_H$  is the mass per hydrogen nucleus. A similar relationship holds for flows controlled by FUV, where the sound speed is of order 1 to 3 km s<sup>-1</sup> and  $r_g$  is correspondingly increased.

Estimating the mass loss rate and dispersal timescale of a disk by photoevaporation therefore reduces to determining  $n_0(r)$ , constrained by the above equations for  $n(r, z)$  and  $H(r)$ , such that the UV photons are just absorbed at the base of the HII atmosphere or flow. For EUV photons, the recombination of electrons and protons in the ionized HII surface layers leads temporarily to H atoms which absorb EUV photons and which then become reionized. Therefore, both dust and recombinations provide a source of opacity which attenuates the incident EUV flux. A self-regulating feedback mechanism is established. The base density  $n_0(r)$  adjusts itself so that EUV photons are nearly completely absorbed by the time they reach the base (i.e., there is an ionization front at the base). If  $n_0(r)$  were lower than this value, the EUV photons would penetrate deeper into the dense neutral disk and would produce a higher  $n_0(r)$ . On the other hand, if the density were higher than this value, then the recombinations or dust in the overlying gas would provide such high opacity that the EUV photons would not penetrate to the base, which is contradictory.

In the case of EUV photons, both the recombinations in the atmosphere and flow as well as the scattering from dust in these regions provide a source of *diffuse* EUV photons. Approximately one third of the recombinations is to the ground state of H, which produces isotropically radiated EUV photons. HJLS94 show that the atmosphere absorbs a significant fraction of the EUV photon luminosity,  $\Phi_i$ , of the central star, and that the diffuse field dominates the direct EUV flux from the star in determining  $n_0(r)$ . In the case of FUV photons, dust scattering alone provides a diffuse source of photons, but this case has not yet been quantitatively analyzed. The dust grains which dominate the scattering and absorption at EUV and FUV wavelengths have typical radii  $\sim 100$  Å. These small dust particles tend to remain in the upper atmospheres of the disks for substantial periods before settling and coagulating (Weidenschilling 1984, see also §IID4). However, if they do clump together and rain out from the upper layers of the disk in the absence of turbulence (cf., Cameron 1995), the scattering could be reduced significantly.

HJLS94 find an analytic solution for the case of EUV photons in the bound ( $r < r_g$ ) region. They find that  $n_0 \propto r^{-3/2}$  in the static region, whereas beyond the static region the power law steepens to  $n(r) \propto r^{-\gamma}$ , where  $\gamma \gtrsim 5/2$ . Most of the mass loss occurs, then, in the

region just outside of  $r_g$ . A complete analysis finds

$$\dot{M}_{ph} = 4 \times 10^{-10} M_{\odot} \text{yr}^{-1} \left( \frac{\Phi_i}{10^{41} \text{s}^{-1}} \right)^{1/2} \left( \frac{M_{\star}}{M_{\odot}} \right)^{1/2}$$

Both within and beyond the static region the ionized hydrogen is maintained primarily from diffuse photons produced in the atmosphere. The dominance of the diffuse field means that the exact shape of the thin disk does not enter (shadowing is not important). In addition, the radiative transfer ensures that  $n_0(r)$  and  $\dot{M}_{ph}$  do not depend on the surface density distribution of the disk, as long as it is sufficient to maintain a dense neutral disk under the HII surface.

Numerical simulations of disks photoionized by a central EUV source with a weak stellar wind have been performed by Yorke & Welz (1994, 1996) and by Richling & Yorke (1997). Richling and Yorke (1997) include the effects of dust scattering and find a similar power law dependence of  $\dot{M}_{ph}$  on  $\Phi_i$  (exponent  $\approx 0.58$ ) and comparable mass loss rates for high mass stars ( $\Phi_i \sim 10^{49} \text{s}^{-1}$ ) in the range  $10^{-7} \lesssim \dot{M}_{ph}/M_{\odot} \text{yr}^{-1} \lesssim 10^{-5.5}$ . However, the numerical simulations employed disks with central holes, whereas the disks discussed here are considered to extend from the stellar surface until  $r \gg r_g$ .

*Strong Stellar Wind Case.* In the case of a strong wind from the central star, the ram pressure of the stellar wind,  $\rho_w v_w^2$ , will be too high for a static atmosphere to achieve a full scale height above the disk. Instead, the stellar wind will suppress the height of the ionized layer out to a radius  $r_w > r_g$ , where the thermal pressure of the ionized hydrogen flowing from the disk balances  $\rho_w v_w^2$  (see Fig. 3b). The photoevaporated material can freely flow vertically off the disk at radii beyond  $r_w \simeq 10 \text{ AU } \dot{M}_{w-10}^2 v_{w7}^2 \Phi_{41}^{-1}$ , where  $\dot{M}_{w-10} = \dot{M}_w / 10^{-10} M_{\odot} \text{yr}^{-1}$ ,  $v_{w7} = v_w / 100 \text{ km s}^{-1}$ , and  $\Phi_{41} = \Phi_i / 10^{41} \text{s}^{-1}$ . The criterion for a strong wind,  $r_w > r_g$ , can be written that the stellar wind mass loss rate  $\dot{M}_w$  exceeds a critical value  $\dot{M}_{cr} = 4 \times 10^{-11} \Phi_{41}^{1/2} M_0^{1/2} v_{w7}^{-1} M_{\odot} \text{yr}^{-1}$ , where  $M_0 = M_{\star} / M_{\odot}$  (HJLS94). Although there are large uncertainties in both  $\dot{M}_w$  and  $\Phi_i$  for young low mass stars, it appears that the strong wind condition may often be met. With fewer uncertainties, it also is generally met for O and B stars (van Buren 1985).

The overall effect of the stellar wind is to allow EUV flux to penetrate more readily to the disk surface in the flow ( $r > r_g$ ) region, which enhances the photoevaporative mass loss rate. HJLS94 find for the strong wind conditions,  $\dot{M}_w > \dot{M}_{cr}$ :

$$\dot{M}_{ph} \simeq 4 \times 10^{-10} M_{\odot} \text{yr}^{-1} \left( \frac{\dot{M}_w}{10^{-10} M_{\odot} \text{yr}^{-1}} \right) \left( \frac{v_w}{100 \text{ km s}^{-1}} \right)$$

The photoevaporative mass loss rate from the outer disk now becomes slightly more than the mass loss rate in the assumed isotropic stellar

wind. We emphasize that these approximate analytical solutions hold only when the disk extends to  $r_d > r_w$ .

The photoevaporation timescale  $t_c(evap)$  caused by the central star in a strong wind case is also plotted in Fig. 1. Here we have assumed that  $r_w > r_d$ , so that  $n_0 \propto r^{-3/2}$  from  $r_g$  to  $r_d$  (HJLS94), and that  $\beta = 3/2$ ,  $\Phi_i = 10^{41} \text{ s}^{-1}$ , and a minimum mass nebula. Since  $\Sigma \propto r^{-3/2}$  is assumed, the photoevaporative timescale becomes independent of  $r$  for  $r > r_g$

$$t_c(evap) \simeq 10^7 \text{ yr} \left( \frac{\Phi_i}{10^{41} \text{ s}^{-1}} \right)^{-1/2} \left( \frac{\Sigma_0}{\Sigma_0(min)} \right),$$

where  $\Sigma_0$  is the disk surface density at a fiducial radius and  $\Sigma_0(min)$  is the corresponding value for the minimum solar nebula.

A strong wind also affects the radiative transfer in two important ways. First, if it is partially neutral, it is a source of opacity for the EUV photons trying to travel from the star to  $r_g$ . Therefore, it could significantly lower the ratio of EUV to FUV photons arriving at  $r_g$  from the star. Secondly, the ionized material in the wind will recombine and thereby produce a “diffuse” source of EUV and FUV photons above the disk. Many of the EUV photons will be absorbed “on the spot” by the neutral component of the wind. These effects should be addressed quantitatively in the future.

Although no analytic solution has been proposed for a central star which radiates only FUV photons, the outline of the solution is clear. In this case dust dominates the opacity. Dust also scatters the FUV (the albedo of interstellar dust is typically  $\sim 0.3 - 0.6$  in the FUV), and the isotropic component of the scattering produces a diffuse FUV field. The critical gravitational radius is now further out, since  $r_g \propto c_S^{-2}$  and the PDR surface gas is cooler than  $10^4$  K. Again, the EUV and FUV flux from the wind should be evaluated.

The above analytic solutions (HJLS94) made simple analytic approximations for the dynamics of an evaporating disk (e.g.,  $v_z = 0$  for  $r < r_g$  and  $v_z = c_S$  for  $r > r_g$ ) and for the radiative transfer solution for the diffuse EUV field. In order to consider various effects such as disk evolution, non-steady state heating/cooling and ionization/recombination as well as more detailed hydrodynamic interactions and radiative transfer, numerical simulations are required.

## 2. Photoevaporation by the central star: numerical simulations

The first numerical simulations of the evolution of circumstellar disks subjected to the influence of EUV photons from the central source were discussed by Yorke & Welz (1993) as a model for UCHII regions. Although the effects of disk rotation, self-gravity, IR heating of the

dust, time dependent heating and cooling, and hydrogen ionization and recombination were included in the 2D axially symmetric hydrodynamic code, these early models considered the direct stellar EUV flux only — sharp shadows were cast by the disk. Including the effects of the diffuse EUV field produced by recombinations directly into the ground state (Yorke & Welz 1994, 1996) allowed the ionization front to wrap around and envelope the disk, but these “soft” EUV photons were able to heat the ionized material in the disk’s shadow regions to  $\approx 2000$  K, much lower than the value  $\approx 8000$  K of the ionized material directly illuminated by the central star. Richling & Yorke (1997) found that by including the effects of UV dust scattering, the “shadow” regions quickly disappeared and the ionized gas attained temperatures  $\approx 8000$  K everywhere. The mass loss rate was enhanced by a factor of about 2 for UV dust opacities  $\kappa_{uv} = 200 \text{ cm}^2 \text{ g}^{-1}$ . Fig. 4 shows results from their numerical simulations. This result is for the case of high mass stars, which produce relatively high ( $\sim 1$ ) dust optical depths in the disk atmosphere. Solar type stars will produce much lower dust optical depths, and will show much less effect from dust scattering.

For the cases with strong stellar winds Yorke & Welz (1996) and Richling & Yorke (1997) find a much weaker dependence of the disk mass loss rate with wind velocity (a power law exponent 0.1 rather than 1) when compared to the analytic models discussed here and by HJLS94. Because, however, the numerical simulations consider cases of very massive disks  $M_d \gtrsim 0.2M_*$  with a central cavity and a finite outer radius  $r_d$  of order  $r_w$ , they are not readily comparable to the analytic results, which assume  $r_d \gg r_w$ . In the numerical simulations the originally isotropic stellar wind interacts with the outflowing photoevaporation flow from the disk to produce shocks in both the wind material and the photoevaporation flow which are separated by a contact discontinuity. The shock heated wind material seeks the easiest path of escape which is along the rotational axis. A hydrodynamically collimated bipolar outflow results, the opening angle of which increases slowly with increasing the wind velocity. For warm ( $T \approx 10^4$  K), low velocity ( $v_w \approx 50 \text{ km s}^{-1}$ ) winds the mass loss rate due to photoevaporation  $\dot{M}_{ph}$  actually *decreases* with increasing stellar wind mass loss  $\dot{M}_w$ , because the wind itself absorbs EUV photons.

### 3. Photoevaporation of the solar nebula by the Sun and the formation of the giant planets

The Introduction presents the current picture of giant planet formation and concludes that 1) this process is a minor disk dispersal mechanism and 2)  $M_d \approx$  several  $M_{\text{min}}$ . As discussed by Shu, Johnstone, & Hollenbach (1993, hereafter SJH93) several serious issues remain in this picture. What dispersed all the residual gas in this enhanced mass

nebula? Removing  $\sim 0.1 M_{\odot}$  of gas stored in a thin disk by a T Tauri wind (mass-loss rate  $\sim 10^{-8} M_{\odot} \text{ yr}^{-1}$  for  $10^7$  yr) is a questionable proposition, whereas transporting this much material inward to the center by viscous accretion would push any planet (like Jupiter) that has cleared a gap around itself also into the sun (for the basic dynamical mechanisms, see Goldreich & Tremaine 1979, 1980; Lin & Papaloizou 1979, 1985; Hourigan & Ward 1984; Ward 1986).

Even if we ignore the timescale problem for accumulating critical cores for the giant planets and assume that the giant planets somehow formed under conditions that resembled the minimum solar nebula, we run into a second difficulty: the delicate timing between core growth and nebula dispersal that must seemingly be achieved to yield the differential results that we observe for the masses of the gaseous envelopes of the four giant planets. The rock-ice cores of the giant planets are all about 15 earth masses ( $M_{\oplus}$ ), but the hydrogen/helium envelopes for Jupiter, Saturn, Uranus, and Neptune contain  $\sim 300$ ,  $\sim 75$ ,  $\sim 2$ , and  $\sim 2 M_{\oplus}$  respectively (SJH93). Note that there is a sharp cut-off in hydrogen/helium mass between Saturn and Uranus, even though the core masses are similar and are presumably large enough in Uranus and Neptune to initiate the rapid accumulation of hydrogen and helium gas. The problem arises because most theories of disk dispersal by thermal evaporation or solar-wind erosion (e.g., Cameron 1978; Elmegreen 1978; Horedt 1978, 1980, 1982; Sekiya et al. 1980; Pechernikova & Vitjazev 1981; Ohtsuki & Nakagawa 1988) predict gas loss-rates that vary smoothly with time and radial position in the disk, whereas the usual core-instability picture demonstrates that the process of runaway gas gathering proceeds very quickly once it gets going. Adjusting the parameters appropriately to explain Jupiter and Neptune will typically leave Uranus and Saturn complete mysteries. The problem then becomes to identify the gas removal mechanism that would satisfactorily explain the sharp differences in envelope masses between the gas-rich giants, Jupiter and Saturn, and the gas-poor giants, Uranus and Neptune.

SJH93 point out an interesting coincidence between  $r_g \approx 10$  AU for the solar system and the radial position which separates the gas-rich giants from the gas-poor. The transition between photoionized gas being gravitationally trapped in the solar nebula and flowing off in an evaporative wind occurs roughly at the orbital distance of Saturn. If the photoevaporative rate of mass loss  $\dot{M}_{ph}$  beyond  $r_g$  is sufficiently large, no hydrogen and helium may be left in the nebula when Uranus and Neptune have acquired large enough core masses to enter the rapid gas-gathering phase.

As we have shown in §IID1 above, the EUV photoevaporative mass loss rate caused by the central star varies as  $\Phi^{1/2}$ . If the photoionization rate  $\Phi_i$  of the primitive sun equals  $10^{41} \text{ s}^{-1}$  for  $\sim 10^7$  yr, an amount of

mass comparable to a minimum solar nebula could have been removed by such a process from the outer disk beyond  $r_g \approx 10$  AU in this period. The rate  $\Phi_i = 10^{41} \text{ s}^{-1}$  exceeds the ultraviolet output of the present sun by two orders of magnitude, but it is compatible with the observed output of CTTSs (see, e.g., Gahm et al. 1979, Bertout 1989). To explain the loss of gases from the Earth's primitive atmosphere by hydrodynamic "blow-off," other workers have postulated EUV rates  $\Phi_i \sim 10^{41} \text{ s}^{-1}$  from the early sun lasting for a few hundred million years (Sekiya et al. 1980; Hunten 1985, 1993; Zahnle & Kasting 1986), so assuming this rate for  $10^7$  yr is conservative in comparison.

Mass accretion from the inner disk onto the stellar surface (Bertout et al. 1988) – possibly aided by magnetic fields (Königl 1991) – may provide the simplest explanation for the ultraviolet excesses of CTTSs. According to the empirical evidence presented by Strom et al. (1989, 1993), the CTTS phase lasts about  $10^7$  yr. If the CTTSs have outer disks that do not contain much more gas than a minimum solar nebula (see, e.g., Beckwith et al. 1990, Terebey et al. 1993), then photoevaporation may well cause the giant planets that form beyond  $r_g$  to be gas-poor giants of the ilk of Uranus and Neptune.

We have discussed in §IID1 that the early sun may have had a strong, partially ionized, wind which may absorb EUV photons from the sun, but which may itself produce an EUV and FUV diffuse field. This effect has not been studied, and may well affect the mass loss rate and to a much lesser extent  $r_g$ . However, the basic point that significant mass loss occurs at a radius outside of Saturn but inside of Uranus remains valid.

SJH93 speculated that the solar nebula actually formed with a mass much greater than the minimum mass. Giant planets that formed early when the outer disk was still massive were pushed by the viscous evolution of the disk into the protosun. Eventually, the combination of viscous accretion and photoevaporation lowered the gas mass exterior to Jupiter's orbit to a value less than a few times Jupiter's mass. At this point, the gas can no longer push the giant planets into the protosun, and the remaining gases are dispersed or accrete onto the giant planets. By this way of thinking, the "minimum solar nebula" does not define the mass of Jupiter, rather the mass of Jupiter defines the conditions of the "protoplanetary" nebula. When the role of photoevaporation is added, this line of thought has the additional noteworthy implication that the resultant disk properties may also automatically produce transitional-case planets like Saturn and gas-poor planets like Uranus and Neptune.

#### 4. Photoevaporation of circumstellar disks by an external star

For low mass stars born in clusters, a significant fraction of the

UV photons incident on the protoplanetary disks may be produced by nearby massive stars and may significantly enhance the photoevaporation process. The “proplyds” (externally-ionized PROtoPLANetary DiskS) in the Orion Nebula are the best example of this scenario and have been extensively studied (Bally et al 1998, O’Dell 1998 and references therein). The Trapezium cluster, whose most massive member  $\theta^1$  Ori C resides at the cluster center and produces the HII region, contains over 700 stars with a peak density of  $5 \times 10^4 \text{ pc}^{-3}$  in the central 0.1 pc diameter core (McCaughrean & Stauffer 1994). Within the HII region over 150 proplyds are visible as small ( $r \lesssim 100 \text{ AU}$ ) ionized envelopes surrounding low mass stars. Churchwell et al (1987), using radio continuum observations, first proposed that evaporating circumstellar disks produced the envelopes. More recently, HST has imaged a number of disks as silhouettes, either against the nebula background (McCaughrean & O’Dell 1996) or against the background ionized envelope (Bally et al 1998). The disks glow in [OI] 6300 Å emission as well (Bally et al 1998).

In Fig. 5 we show two narrow band images of proplyd HST 182-413 (HST 10). The head-tail appearance is characteristic of *all* proplyds, with the head pointing toward  $\theta^1$  Ori C (although not always exactly). HST 182-413 contains a disk ( $r_d \simeq 100 \text{ AU}$ ) visible as an edge-on silhouette in all filters except [O I] and  $H_2$  (Chen et al 1998), where the disk emits. Surrounding the disk, yet well offset, is an envelope of ionized gas. In the case of HST 182-413, neutral material is removed from the disk surface at a rate higher than the incident EUV flux can keep entirely ionized, producing the offset ionization front.

In this section we discuss the photoevaporation of circumstellar disks by external stars using the Orion Nebula observations as a guide. The first assumption made in models of externally illuminated disks is that the disk radius  $r_d > r_g$ , so that evaporation occurs. For externally illuminated disks, this means that  $r_g$  effectively drops out of the problem. The incident EUV or FUV flux sets up a flow of constant mass flux from the disk surface for  $r > r_g$ . In contrast to photoevaporative flows caused by the central star, where the mass loss was dominated by the *inner*  $r \sim r_g$  or  $r_w$  region close to the source, the mass loss for external illumination is dominated by the *outer*  $r \sim r_d$  region, where most of the surface area lies.

Since most of the mass loss is from  $r \sim r_d$ , the evaporation from the disk can be approximated by the evaporation from a sphere of radius  $r_d$ . Pressure gradients in the flow will cause the streamlines to rapidly diverge beyond  $r_d$  and approximate spherical outflow. The “surface” of the disk (sphere), for the purposes of photoevaporation, can be defined as the sonic surface where the disk flow transitions from subsonic to supersonic flow. As discussed in §IID1, it lies at the point where the EUV or FUV flux is attenuated to the point of just heating the gas

to a temperature such that the sound speed equals the escape speed. If EUV dominates at the sonic point, either dust or recombinations can attenuate the flux. If FUV dominates, then dust is the prime opacity source. Let  $n_0$  be the gas density at the disk surface or sonic point. Then the photoevaporative mass loss from the sphere is given  $\dot{M}_{ph} \simeq m_H n_0 c_S 4\pi r_d^2$ , where  $c_S$  is the sound speed in the heated ( $10^4$  K ionized or  $\sim 10^3$  K neutral) flow. Therefore, to calculate  $\dot{M}_{ph}$ , one need only estimate  $n_0$ . The base density  $n_0$  is given by the condition that the EUV or FUV be (just) absorbed in the flow.

If dust dominates the EUV or FUV opacity, then the dust optical depth  $\tau_{UV}$  in the flow is proportional to the gas column density  $N_D$  in the flow. Because the density falls off rapidly due to spherical divergence,  $N_D \simeq n_0 r_d$ . For interstellar dust,  $N_D \simeq 10^{21}$  cm $^{-2}$  gives  $\tau_{UV} \simeq 1$ . Given that  $N_D$  is fixed to give  $\tau_{UV} \sim \text{few}$ , it follows  $n_0 \propto r_d^{-1}$ ; the base density is smaller for larger disks. In the case  $n_0 r_d \sim \text{constant}$ ,  $\dot{M}_{ph}$  is quite independent of the incident UV flux (as long as it is sufficient to heat the gas so that  $c_S \sim \text{constant}$ ), and  $\dot{M}_{ph} \propto r_d$ .

If recombinations dominate the EUV opacity, then the recombinations in a radial column,  $\sim (1/3)\alpha_r n_0^2 r_d$ , where  $\alpha_r$  is the recombination coefficient for  $10^4$  K ionized gas, balance the incident EUV flux  $F_i = \Phi_i / (4\pi d^2)$ , where  $d$  is the distance to the EUV source. In this case,  $\dot{M}_{ph}$  depends on the incident EUV flux ( $\dot{M}_{ph} \propto F_i^{1/2}$ ) and  $\dot{M}_{ph} \propto \Phi_i^{1/2} d^{-1} r_d^{3/2}$ .

Johnstone, Hollenbach & Bally (1998, hereafter JHB98) and Störzer & Hollenbach (1999, hereafter SH99) showed that the photoevaporation rates of disks around low mass stars illuminated by nearby massive stars may either be dominated by the EUV or the FUV photon flux from the high mass star. In the case of EUV-dominated flow, a thin PDR region ( $\Delta r \lesssim r_d$ ) is produced at the disk surface by the FUV flux, but the neutral gas moves subsonically through the PDR to the ionization front (IF), where the flow is ionized, heated to  $10^4$  K, and accelerated to supersonic speeds,  $v_f \gtrsim 10$  km s $^{-1}$ . The mass loss rate, if recombinations dominate the opacity, is given from the above

$$\dot{M}_{ph}^{EUV} \simeq 7 \times 10^{-9} M_{\odot} \text{yr}^{-1} \left( \frac{\Phi_i}{10^{49} \text{ s}^{-1}} \right)^{1/2} \left( \frac{r_d}{10 \text{ AU}} \right)^{3/2} \left( \frac{10^{17} \text{ cm}}{d} \right),$$

where  $\Phi_i \sim 10^{49}$  s $^{-1}$  for an early O star as nearby neighbor.

On the other hand, in FUV-dominated flows, the FUV produces sufficient PDR pressure that a supersonic neutral flow is launched from the disk surface. The ionizing EUV flux cannot penetrate this opaque flow until its density has dropped significantly. The ionized HII flow commences at an IF at a standoff distance  $r_{IF} \gtrsim 2r_d$ . Moving outwards from the disk surface, the supersonic neutral wind first passes through

a shock, decelerates to subsonic speeds, forms a thick subsonic layer, and then passes through a D-type stationary IF at  $r_{IF}$  where the flow is heated to  $10^4$  K and reaccelerated to supersonic ( $v_f \gtrsim 10$  km s $^{-1}$ ) speeds. The mass loss rate in this case can be approximated

$$\dot{M}_{ph}^{FUV} \simeq 2 \times 10^{-8} M_{\odot} \text{ yr}^{-1} \left( \frac{N_D}{5 \times 10^{21} \text{ cm}^{-2}} \right) \left( \frac{r_d}{10 \text{ AU}} \right),$$

where  $N_D$  ( $\sim 5 \times 10^{21}$  cm $^{-2}$  in the numerical studies of SH99) is the column density from the ionization front to the sonic point (disk surface).

Given the UV flux incident upon the disk and the disk size  $r_d$ , the photoevaporation model predicts  $r_{IF}$ , with only one “free” parameter, the UV opacity of the dust grains in the flow. Approximately 10 proplyds have been observed in Orion where both  $r_d$  and  $r_{IF}$  are directly measured with some accuracy (JHB98). SH99 used these sources to derive an average UV dust opacity in the evaporating flows and found a dust cross section per hydrogen nucleus of  $\sigma_{UV} \simeq 8 \times 10^{-22}$  cm $^2$ . This value is only a factor of 2 or 3 less than diffuse interstellar values, and compatible with Orion nebula or dense molecular cloud values (Draine & Bertoldi 1996). Therefore, consistent with the expectations of settling and coagulation of dust particles in disks (Weidenschilling 1984; Weidenschilling & Cuzzi 1993), the abundance of small ( $\sim 100$  Å) dust particles which dominate the UV opacity is relatively unchanged in the upper atmospheres of these young ( $t \lesssim 10^6$  yr) disks at 10-100 AU.

Using this value for  $\sigma_{UV}$ , SH99 derive the parameter space for EUV and FUV-dominated flows for the proplyds in Orion. FUV-dominated flows occur roughly when  $10 \text{ AU} \lesssim r_d \lesssim 100 \text{ AU}$  and when  $0.01 \text{ pc} \lesssim d \lesssim 0.3 \text{ pc}$ , where  $d$  is the distance to the dominant UV source  $\theta^1$  Ori C. For large distances or small disks, the FUV cannot heat the PDR to sufficient temperature to drive evaporative flow (i.e.,  $c_S < v_{\text{escape}}$ ). For small distances or large disks, the EUV penetrates close to the disk surface and determines the mass loss.

JHB98 and SH99 analyzed the observational data from approximately 40 proplyds and showed that many of the flows are likely to be FUV-dominated. Störzer & Hollenbach (1998) and SH99 further showed that the FUV-dominated flow models match perfectly with the observed intensities of the optical emission near the IF as well as the neutral [OI] 6300 Å and H $_2$  2  $\mu\text{m}$  intensities coming from the disk surface. Henney & Arthur (1998) show that a photoevaporation model fits the observed fall-off in optical emission with distance from the proplyd. JHB98 proposed that the observed tails of the comet-shaped ionization fronts could be caused by the diffuse UV radiation driving an FUV-dominated flow from the shadowed side of the proplyd. Fig. 6

shows a numerical confirmation of this proposal from Richling & Yorke (1998b). The numerical study used such a large disk ( $r_d \sim 300$  AU) that the front side is EUV-dominated. Nevertheless, on the back side an FUV-dominated flow with an IF shaped like the observed tails is seen in the simulation. All these results give added confidence in the validity of the FUV-dominated photoevaporation models.

Assuming that  $\sigma_{UV}$  is approximately the same for all the observed proplyds, the theoretical models are able to predict the disk sizes from the observed sizes of the ionization fronts. JHB98 derived the disk sizes for approximately 30 proplyds where  $r_{IF}$  was measured but where the disk could not be seen. The disk sizes ranged from 10–100 AU.

If the proplyds are in circular orbits around the UV source  $\theta^1$  Ori C so that  $d$  is constant in time, JHB98 and SH99 showed how the current disk mass  $M_d$  could be estimated from the current  $\dot{M}_{ph}$  and the disk illumination time  $t_i$ . Assuming that the surface density in the disk scales as  $\Sigma \propto r^{-\beta}$  where  $1 < \beta < 2$ , most of the mass in the disk is at  $r \sim r_d$ , the disk evaporates from outside in, and the timescale for evaporation  $t_{evap}$  increases as the disk shrinks. (Note that  $t_{evap} = M_d/\dot{M}_{ph}$  is not the timescale for complete dispersal, but only for the mass and radius to decrease by factors of order 2). If the disks initially are large enough that they have shrunk significantly after time  $t_i$ ,  $M_d \simeq \dot{M}_{ph} t_i$ . Millimeter observations (Lada 1998) detect two disks with  $M_d \sim 0.01 M_\odot$  and limit several others to smaller masses. Observed and theoretical estimates (JHB98, SH99) of  $\dot{M}_{ph} \gtrsim 10^{-7} M_\odot \text{ yr}^{-1}$  then limit  $t_i < 10^5$  yr. In the case of circular orbits, it appears that  $\theta^1$  Ori C must be less than  $10^5$  years old, surprisingly small compared to the  $\sim 10^6$  yr age estimated for the low mass stars in the cluster (Hillenbrand 1997).

On the other hand, the proplyds are likely to be on much more eccentric orbits around  $\theta^1$  Ori C. (Note that the cluster potential is dominated by the distributed mass for  $d \gtrsim 0.05$  pc, so the orbits are not Keplerian in any case). SH99 considered the opposite extreme of radial orbits and showed that, in this case, the disks may shrink and lose mass as they approach  $\theta^1$  Ori C. However, inside a critical distance  $d_{cr}$ , their dynamical time is shorter than  $t_{evap}$  and so they move quickly through the central region “frozen” in mass and size. For disks which have experienced significant shrinkage and which lie inside of  $d_{cr}$  (as most of the  $\sim 40$  well-studied proplyds do), the current mass of the disk is approximately  $M_d \simeq \dot{M}_{ph}(d_{cr}/v)$ , where  $\dot{M}_{ph}$  is evaluated at  $d_{cr}$  and where  $d_{cr}/v$  is the crossing time  $t_c$  for a proplyd moving at  $v$  through the central region. Hillenbrand (1997) estimates  $v \simeq 2.3 \text{ km s}^{-1}$ , or  $t_c \simeq 10^5$  yr. SH99 derive theoretically that  $d_{cr} \simeq 0.2$  pc and that  $\dot{M}_{ph}$  at  $d_{cr}$  is roughly fitted by the analytic approximation to numerical models  $\dot{M}_{ph} \simeq 10^{-7} (r_d/100 \text{ AU})^{1-1.5} M_\odot \text{ yr}^{-1}$ . Therefore, the disk masses for shrunken proplyds passing near ( $d < d_{cr}$ )  $\theta^1$  Ori C

are given  $M_d \simeq 10^{-2}(r_d/100\text{AU})^{1-1.5} M_\odot$ ; the disk masses are roughly proportional to their sizes. Since most of the 40 well-studied proplyds have  $r_d \lesssim 100$  AU, the models predict  $M_d \lesssim 10^{-2} M_\odot$ , in agreement with observation. In this case of radial orbits, there is no need for  $\theta^1\text{Ori C}$  to be exceptionally young. The Trapezium cluster extends to  $d \sim 2$  pc, has a half mass radius of  $d \sim 0.5$  pc, and a typical crossing time across the whole cluster of  $\sim 10^6$  yr (Hillenbrand 1997). If  $\theta^1\text{Ori C}$  is  $\sim 10^6$  years old and the entire cluster is on radial orbits, then each of the  $\sim 1000$  proplyds in the cluster has passed close to  $\theta^1\text{Ori C}$  roughly one time, and has photoevaporated to  $r_d \sim 10 - 100$  AU. We presently observe mostly the nearby bright objects inside of  $d_{cr}$ . Those foreground proplyds which have not passed through the central regions and which have stayed outside ( $d \gtrsim 0.6 - 1$  pc) the HII region, perhaps because their orbits are more circular, remain large ( $r_d \sim 100 - 500$  AU) and are observed as silhouettes (McCaughrean & O'Dell 1996). In the case of the Trapezium cluster, one O star has significantly affected the disk evolution of perhaps hundreds of low mass stars like the sun through the process of photoevaporation.

Although it appears that most stars in the Galaxy are formed in clusters (Lada et al 1991, Lada 1992, Bonnell & Kroupa 1998) and that these clusters have sizes 0.1 - 1 pc, it is not clear how many stars form in a typical cluster. If that number is greater than about 100, then it is very likely that an O or B star will form among its members, and that photoevaporation by an external star will affect the fate of most planet-forming disks in the Galaxy. In Fig. 1 we have also plotted the photoevaporation timescale  $t_E(\text{evap})$  as a function of  $r$  for disks around low mass stars in clusters like the Trapezium cluster.

### III. CONCLUSIONS

Fig. 1 shows the timescales for various gas (and small dust) dispersal mechanisms in planet-forming disks as a function of the position  $r$  in the disk. The stellar encounter lifetime  $t_{SE}$  is plotted for Trapezium-like conditions ( $n_* = 10^4 \text{ pc}^{-3}$  and  $v = 1 \text{ km s}^{-1}$ ) and is clearly only important in the outer regions  $r \gtrsim 100$  AU of planet-forming disks in dense clusters. The viscous timescale  $t_\nu$  is plotted for two representative values of  $\alpha$ , and are seen to be dominant in the inner,  $r < 10$  AU, parts of disks. The wind timescales,  $t_{ws}$  and  $t'_{ws}$ , are plotted assuming a minimum mass ( $M_d \simeq 0.01 M_\odot$ ) disk with  $\beta = 3/2$  and with  $\epsilon(\sin\theta)^2 = 10^{-4}$ . Wind mass loss rates of  $\dot{M}_w = 10^{-8} M_\odot \text{ yr}^{-1}$  are assumed for  $t_{ws}$ ; in the  $t'_{ws}$  case, we have assumed that the wind mass loss rate declines with time as  $\dot{M}_w = 10^{-6}(10^5 \text{ yr}/t) M_\odot \text{ yr}^{-1}$  for  $t < 10^7$  yr. The winds are assumed to be spherically symmetric. Although there is considerable uncertainty in  $\epsilon \sin\theta$ , it appears that stellar wind stripping is not particularly effective, in contrast to the commonly held view

of the dispersal of the solar nebula. The photoevaporation timescale  $t_c(\text{evap})$  caused by the central star is plotted assuming  $\Phi_i = 10^{41} \text{ s}^{-1}$ , the “strong wind” case, and a minimum mass nebula with  $\beta = 3/2$ . The photoevaporation timescale  $t_E(\text{evap})$  caused by an external star is plotted for Trapezium conditions, assuming radial orbits, a cluster of size 1 pc, and a minimum mass nebula with  $\beta = 3/2$ . The photoevaporation timescales become very long at  $r < 10 \text{ AU}$  because the stellar gravity holds the disk material and prevents evaporation. Photoevaporation is generally dominant for  $r > 10 \text{ AU}$ .

The rapid cutoff between Saturn and Uranus in the hydrogen and helium gas content of the giant planets may be explained by the photoevaporation of the outer,  $r > 10 \text{ AU}$ , early solar nebula before Uranus and Neptune could accumulate the gas. SJH93 proposed that the early sun provided the UV photons. However, it is also quite possible that the solar nebula could have spent its early life in a stellar cluster where a nearby O or B star may have photoevaporated the outer nebula in timescales  $t \lesssim 10^7$  years.

### Acknowledgements

This work has been supported in part through the NASA Astrophysics Theory Program which supports a joint Center for Star Formation Studies at NASA/Ames Research Center, UC Berkeley, and UC Santa Cruz, in part through NASA funding at JPL within the “Origins” Program, and in part through funding by the Natural Sciences and Engineering Research Council of Canada.

## REFERENCES

- Adams, F. C., Emerson, J. P., & Fuller, G. A., 1990, Submillimeter photometry and disk masses of T Tauri disk systems, *ApJ*, 357, 606
- Balbus, S. A. & Hawley, J. F., 1991, A powerful local shear instability in weakly magnetized disks. I - Linear analysis. II - Nonlinear evolution, *ApJ*, 376, 214
- Bally, J. & Scoville, N. Z., 1982, Structure and evolution of molecular clouds near H II regions. II - The disk constrained H II region, *S106, ApJ*, 255, 497
- Bally, J., Sutherland, R. S., Devine, D., & Johnstone, D., 1998, Externally Illuminated Young Stellar Environments in the Orion Nebula: Hubble Space Telescope Planetary Camera and Ultraviolet Observations, *AJ*, 116, 293
- Beckwith, S. V. W., Sargent, A. I., Chini, R. S., & Guesten, R., 1990, A survey for circumstellar disks around young stellar objects, *AJ*, 99, 924
- Bertout, C., 1989, T Tauri stars - Wild as dust, *ARAA*, 27, 351
- Bertout, C., Basri, G., & Bouvier, J., 1988, Accretion disks around T Tauri stars, *ApJ*, 330, 350
- Bodenheimer, P. & Pollack, J. B., 1986, Calculations of the accretion and evolution of giant planets: The effects of solid cores, *Icarus*, 67, 391
- Bonnell, I. & Kroupa, P., 1998, Dynamical interactions in dense stellar clusters, in *The Orion Complex Revisited* (M.J. McCaughrean & A. Burkert, Eds), ASPCS, in press
- Burrows, C. J., Stapelfeldt, K. R., Watson, A. M., et al, 1996, Hubble Space Telescope Observations of the Disk and Jet of HH 30, *ApJ*, 473, 437
- Cameron, A. G. W., 1973, Accumulation processes in the primitive solar nebula, *Icarus*, 18, 407
- Cameron, A. G. W., 1978, Physics of the primitive solar nebula and of giant gaseous protoplanets, in *Protostars and Planets*, U. Ariz. Press, pp. 453
- Cameron, A. G. W., 1995, The first ten million years in the solar nebula, *Meteoritics*, 30, 133
- Canto, J. & Raga, A., 1991, Mixing layers in stellar outflows, *ApJ*, 372, 646
- Chen, H., Bally, J., O'Dell, C. R., McCaughrean, M. J., Thompson, R. L., Rieke, M., Schneider, G., Young, E. T., 1998, 2.12 micron molecular hydrogen emission from circumstellar disks embedded in the Orion Nebula, *ApJL*, 492, L173
- Churchwell, E., Felli, M., Wood, D. O. S., Massi, M., 1987, Solar system

- sized condensations in the Orion Nebula, *ApJ*, 321, 516
- Clarke, C. J. & Pringle, J. E., 1993, Accretion disc response to a stellar fly-by, *MNRAS*, 261, 190
- Draine, B. T. & Bertoldi, F., 1996, Structure of stationary photodissociation fronts, *ApJ*, 468, 269
- Elmegreen, B. G., 1978, On the interaction between a strong stellar wind and a surrounding disk nebula, *M&P*, 19, 261
- Elmegreen, B. G., 1979, On the disruption of a protoplanetary disk nebula by a T Tauri like solar wind, *A&A*, 80, 77
- Gahm, G. F., Fredga, K., Liseau, R., & Dravins, D., 1979, The far-UV spectrum of the T Tauri star RU Lupi, *AAP*, 73, L4
- Goldreich, P., Tremaine, S., 1979, The excitation of density waves at the Lindblad and corotation resonances by an external potential, *ApJ*, 233, 857
- Goldreich, P., Tremaine S., 1980, Disk-satellite interactions, *ApJ*, 241, 425
- Greenberg, R., Hartmann, W. K., Chapman, C. R., Wacker, J. F., 1978, Planetesimals to planets - Numerical simulation of collisional evolution, *Icarus*, 35, 1
- Greenberg, R., Weidenschilling, S., Chapman, C. R., Davis, D. R., 1984, From icy planetesimals to outer planets and comets, *Icarus*, 59, 87
- Hall, S. M., Clarke, C. J., Pringle, J. E., 1996, Energetics of star-disc encounters in the non-linear regime, *MNRAS*, 278, 303
- Hartmann, L., Calvet, N., Gullbring, E., D'Alessio, P., 1998, Accretion and the evolution of T Tauri disks, *ApJ*, 495, 385
- Hayashi, C., Nakazawa, K., Nakagawa, Y., 1985, Formation of the solar system, in *Protostars and Planets II*, U. Ariz. Press, pp. 1100
- Heller, C. H., 1995, Encounters with protostellar disks. II. Disruption and binary formation, *ApJ*, 455, 252
- Henney, W. J. & Arthur, S. J., 1998, Modeling the brightness profiles of the Orion proplyds, *AJ*, 116, 322
- Hillenbrand, L., 1997, On the stellar population and star-forming history of the Orion Nebula Cluster, *AJ*, 113, 1733
- Hollenbach, D., Johnstone, D., & Shu, F., 1993, Photoevaporation of disks around massive stars and ultracompact HII regions, in *Massive Stars: Their Lives in the Interstellar Medium*, (J. P. Cassinelli and E. B. Churchwell, Eds.), ASPCS 35, 26
- Hollenbach, D., Johnstone, D., Lizano, S., Shu, F., 1994, Photoevaporation of disks around massive stars and application to ultracompact H II regions, *ApJ*, 428, 654
- Hollenbach, D., Tielens A. G. G. M., 1997, Dense Photodissociation Regions (PDRs) *ARAA*, 35, 179
- Horedt, G. P., 1978, Blow-off of the protoplanetary cloud by a T-Tauri like solar wind, *AAP*, 64, 173

- Horedt, G. P., 1980, Mass loss from planetary protoatmospheres and from the protoplanetary nebula, AAP, 92, 267
- Horedt, G. P., 1982, Mass loss from the protoplanetary nebula, AAP, 110, 209
- Hourigan, K. & Ward, W. R., 1984, Radial migration of preplanetary material - Implications for the accretion time scale problem, Icarus, 60, 29
- Hunten, D. M., 1985, Blowoff on an atmosphere and possible application to Io, Geophys. Res. Lett., 12, 271
- Hunten, D. M., 1993, Atmospheric evolution of the terrestrial planets, Science, 259, 915
- Johnstone, D., Hollenbach, D., & Bally, J., 1998, Photoevaporation of disks and clumps by nearby massive stars: application to disk destruction in the Orion Nebula, ApJ, 499, 758
- Kepler, J., Hartigan, P., Yang, C., & Strom, S., 1993, Hubble Space Telescope images of the subarcsecond jet in DG Tauri, ApJL, 415, L119
- Kessel, O., Richling, S., Yorke, H. W., 1998, Photoevaporation of protostellar disks. III. The appearance of photoevaporating disks around young intermediate stars, A&A, 337, 832.
- Koerner, D. W., Sargent, A. L., & Beckwith, S. V. W., 1993, A rotating gaseous disk around the T Tauri star GM Aurigae., Icarus, 106, 2
- Königl, A., 1991, Disk accretion onto magnetic T Tauri stars, ApJL, 39
- Königl, A., 1995, Disk-driven hydromagnetic winds in young stellar objects, RMxAC, 1, 275
- Lada, E. A., 1992, Global star formation in the L1630 molecular cloud, ApJL, 393, L25
- Lada, E. A., Evans, N. J., DePoy, D. L., Gatley, I., 1991, A 2.2 micron survey in the L1630 molecular cloud, ApJ, 371, 171
- Lada, E. A. 1998, Observations of star formation: the role of embedded clusters, in *Origins*, C. E. Woodward, J. M. Shull, & H. A. Thronson, Eds, (ASP Publishing: San Francisco), p198
- Larwood, J. D., 1997, The tidal disruption of protoplanetary accretion discs, MNRAS, 290, 490
- Laughlin, G., Bodenheimer P., 1994, Nonaxisymmetric evolution in protostellar disks, ApJ, 436, 335
- Lin, D. N. C., Bodenheimer P., Richardson D. C., 1996, Orbital migration of the planetary companion of 51 Pegasi to its present location, Nature, 380, 606
- Lin, D. N. C., Papaloizou, J., 1979, Tidal torques on accretion discs in binary systems with extreme mass ratios, MNRAS, 186, 799
- Lin, D. N. C. & Papaloizou, J., 1985, On the dynamical origin of the solar system, Protostars and Planets, 981
- Lin, D. N. C. & Papaloizou, J., 1986, On the tidal interaction between

- protoplanets and the primordial solar nebula. II - Self-consistent nonlinear interaction, *ApJ*, 307, 395
- Lin, D. N. C. & Papaloizou, J., 1986, On the tidal interaction between protoplanets and the protoplanetary disk. III - Orbital migration of protoplanets, *ApJ*, 309, 846
- Lissauer, J. J., 1987, Timescales for planetary accretion and the structure of the protoplanetary disk, *Icarus*, 69, 249
- Lissauer, J. J., 1993, Planet formation, *ARAA*, 31, 129.
- McCaughrean, M. J., O'Dell C. R., 1996, Direct Imaging of Circumstellar Disks in the Orion Nebula, *AJ*, 111, 1977
- McCaughrean, M. J. & Stauffer, J. R., 1994, High resolution near-infrared imaging of the Trapezium: A stellar census, *AJ*, 106, 1382
- Mizuno, H., 1980, Formation of the giant planets, *Prog.Theor.Phys.*, 64, 544
- Nakagawa, Y., Hayashi, C., & Nakazawa, K., 1983, Accumulation of planetesimals in the solar nebula, *Icarus*, 54, 361
- O'Dell, C. R., 1998, Observational properties of the Orion Nebula proplyds, *AJ*, 115, 263
- Ohtsuki, K., Nakagawa Y., 1988, Accumulation process of planetesimals to the planets, *Prog.Theor.Phys.Suppl.*, 96, 239
- Ouyed, R. & Pudritz, R., 1997a, Numerical simulations of astrophysical disks. I. Stationary models, *ApJ*, 482, 712
- Ouyed, R. & Pudritz, R., 1997b, Numerical simulations of astrophysical disks. II. Episodic outflows, *ApJ*, 484, 794
- Papaloizou, J. & Lin, D. N. C., 1984, On the tidal interaction between protoplanets and the primordial solar nebula. I - Linear calculation of the role of angular momentum exchange, *ApJ*, 285, 818
- Pechernikova, G. V., Vitjazev A. V., 1981, in *Workshop on comparative studies of planetary interiors*, *Adv.Sp.Research*, 1, 55.
- Pollack, J. B., Hubickyj O., Bodenheimer P., Lissauer J. J., Podolak M., Greenzweig Y., 1996, Formation of the giant planets by concurrent accretion of solids and gas, *Icarus*, 124, 62
- Pringle, J. E., Rees, M. J., 1972, Accretion disc models for compact X-ray sources, *A&A* 21, 1
- Richling, S., Yorke, H. W., 1997, Photoevaporation of protostellar disks. II. The importance of UV dust properties and ionizing flux, *A&A*, 327, 317
- Richling, S., Yorke, H. W., 1998a, Photoevaporation of protostellar disks III. The appearance of photoevaporating disks around young intermediate mass stars, *A&A*, in press
- Richling, S., Yorke, H. W., 1998b, Photoevaporation of protostellar disks IV. Circumstellar disks under the influence of both EUV and FUV, in prep.
- Safronov, V. S., 1969, *Evolution of the protoplanetary cloud and formation of Earth and the planets*, Nauka, Moscow.

- Sekiya, M., Nakazawa, K., Hayashi, C., 1980, Dissipation of the rare gases contained in the primordial earth's atmosphere, *E&P Sci. Lett.*, 50, 197
- Shakura, N. I., Sunyaev, R. A., 1973, Black holes in binary systems. Observational appearance, *A&A*, 24, 337
- Shu, F. H., Johnstone, D., Hollenbach, D., 1993, Photoevaporation of the solar nebula and the formation of the giant planets, *Icarus*, 106, 92
- Shu, F. H., Lizano, S., Ruden, S. P., Najita, J., 1988, Mass loss from rapidly rotating magnetic protostars, *ApJ*, 328, L19
- Stapelfeldt, K. R., Burrows, C. J., Krist, J., et al, 1994, WFPC2 Observations of the HH 30 disk and jet, *BAAS*, 185, 4802
- Störzer, H., Hollenbach, D., 1998, On the [O I] lambda 6300 line emission from the photoevaporating circumstellar disks in the Orion Nebula, *ApJ*, 502, 71
- Störzer, H., Hollenbach, D., 1999, PDR models of photoevaporating circumstellar disks and application to the proplyds in Orion, *ApJ*, in press
- Strom, K. M., Strom, S. E., Edwards, S., Cabrit, S., Skrutskie, M. F., 1989, Circumstellar material associated with solar-type pre-main-sequence stars - A possible constraint on the timescale for planet building, *AJ*, 97, 1451
- Strom, S. E., Edwards, S., Skrutskie, M. F., 1993, Evolutionary time scales for circumstellar disks associated with intermediate- and solar-type stars, in *Protostars and Planets III*, p. 837
- Strom, S. E., 1995, Initial Frequency, Lifetime and Evolution of YSO Disks, *RevMexAA*, 1, 317
- Terebey, S., Chandler, C. J., Andr'e, P., 1993, The contribution of disks and envelopes to the millimeter continuum emission from very young low-mass stars, *ApJ*, 414, 759
- Terebey, S., Shu, F. H., & Cassen, P., 1984, The collapse of the cores of slowly rotating isothermal clouds, *ApJ*, 286, 529
- van Buren, D., 1985, The initial mass function and global rates of mass, momentum, and energy input to the interstellar medium via stellar winds, *ApJ*, 294, 567
- Ward, W. R., 1986, Density waves in the solar nebula - Differential Lindblad torque, *Icarus*, 67, 164
- Weidenschilling, S. J., 1984, Evolution of grains in a turbulent solar nebula, *Icarus*, 60, 553
- Weidenschilling, S. J., Cuzzi, J. N., 1993, Formation of planetesimals in the solar nebula, in *Protostars and Planets III*, pp. 1031
- Wetherill, G. W., 1980, Formation of the terrestrial planets, *ARAA*, 18, 77
- Wetherill, G. W., Stewart, G. R., 1986, The early stages of planetesimal accumulation, *L&PS* 17, 939

- Wood, D. O. S., Churchwell, E., 1989, The morphologies and physical properties of ultracompact H II regions, *ApJS*, 69, 831
- Yorke H. W., Bodenheimer P., Laughlin G., 1995, The formation of protostellar disks. 2: Disks around intermediate-mass stars, *ApJ*, 443, 199
- Yorke, H. W., Welz, A., 1993, in *Star Formation, Galaxies and the Interstellar Medium*, eds. J. Franco et al, Cambridge U. Press, pp. 239
- Yorke, H. W., Welz, A., 1994, in *Numerical Simulations in Astrophysics*, eds. J. Franco et al., Cambridge U. Press, pp. 318
- Yorke, H. W., Welz, A., 1996, Photoevaporation of protostellar disks. I. The evolution of disks around early B stars, *A&A* 315, 555
- Zahnle, K .J., Kasting, J. F., 1986, Mass fractionation during transonic escape and implications for loss of water from Mars and Venus, *Icarus*, 68, 462

## FIGURE CAPTIONS

- Figure 1. Timescales for disk dispersal:  $t_\nu$  is the viscous timescale for  $\alpha = 10^{-2}$  and  $10^{-3}$ ;  $t_{SE}$  is the stellar encounter (tidal stripping) timescale for Trapezium cluster conditions (see §III);  $t_{ws}$  and  $t'_{ws}$  are stellar wind stripping timescales for wind and disk parameters summarized in §III;  $t_c(evap)$  is the photoevaporation timescale by the central star (strong wind case) and  $t_E(evap)$  is the photoevaporation timescale for an external star (Trapezium conditions) for the conditions summarized in §IID and §III.
- Figure 2. Schematic representations of the stripping of disk material due to the shear caused by the impact of a stellar wind.
- Figure 3. Schematic representation of photoevaporation by the central star. On the top (a) is the case with insignificant stellar wind. On the bottom (b) is the strong wind case. The scale height  $H(r)$  of the disk is shown in (a), along with typical paths of direct and diffuse EUV photons.
- Figure 4. Numerical simulations of the photoionization and photoevaporation of circumstellar disks by a central EUV source (Richling & Yorke 1997). Top: density (grey scale + contours), ionization front (thick line) and velocity structure (defined at tips of arrows – the velocity scale is given at the upper right of each frame) are shown long after a quasi-steady state flow has been achieved. Middle: the corresponding temperature structure is displayed. Bottom: the resulting quasi-steady state structure of a simulation which included the effects of a central stellar wind (Kessel et al 1998).
- Figure 5. Hubble Space Telescope images of HST 182-413 (HST 10) in  $H\alpha$  (left) and [O I] 6300 Å (right). The disk appears in absorption for most optical lines except [O I]. The ionization front, seen clearly in  $H\alpha$  is offset from the disk surface (JHB98).
- Figure 6. Numerical simulations of the photoionization and photoevaporation of circumstellar disks by an external EUV+FUV source (Richling & Yorke 1998b). The top frame depicts an early stage after the sudden turn-on of the source located above the disk with fluxes:  $f_{EUV} = 6.3 \times 10^{12} \text{ cm}^{-2} \text{ s}^{-1}$  and  $f_{FUV} = 1.6 \times 10^{13} \text{ cm}^{-2} \text{ s}^{-1}$ . The appearance at this time of a second simulation with a higher FUV flux  $f_{FUV} = 1.3 \times 10^{14} \text{ cm}^{-2} \text{ s}^{-1}$  is nearly identical. The bottom frame shows the quasi-steady state result of this simulation. Note the significant reduction of disk size due to removal of the loosely bound outer disk material. The FUV-dominated flow on the back side creates a comet-like tail.

Fig. 1

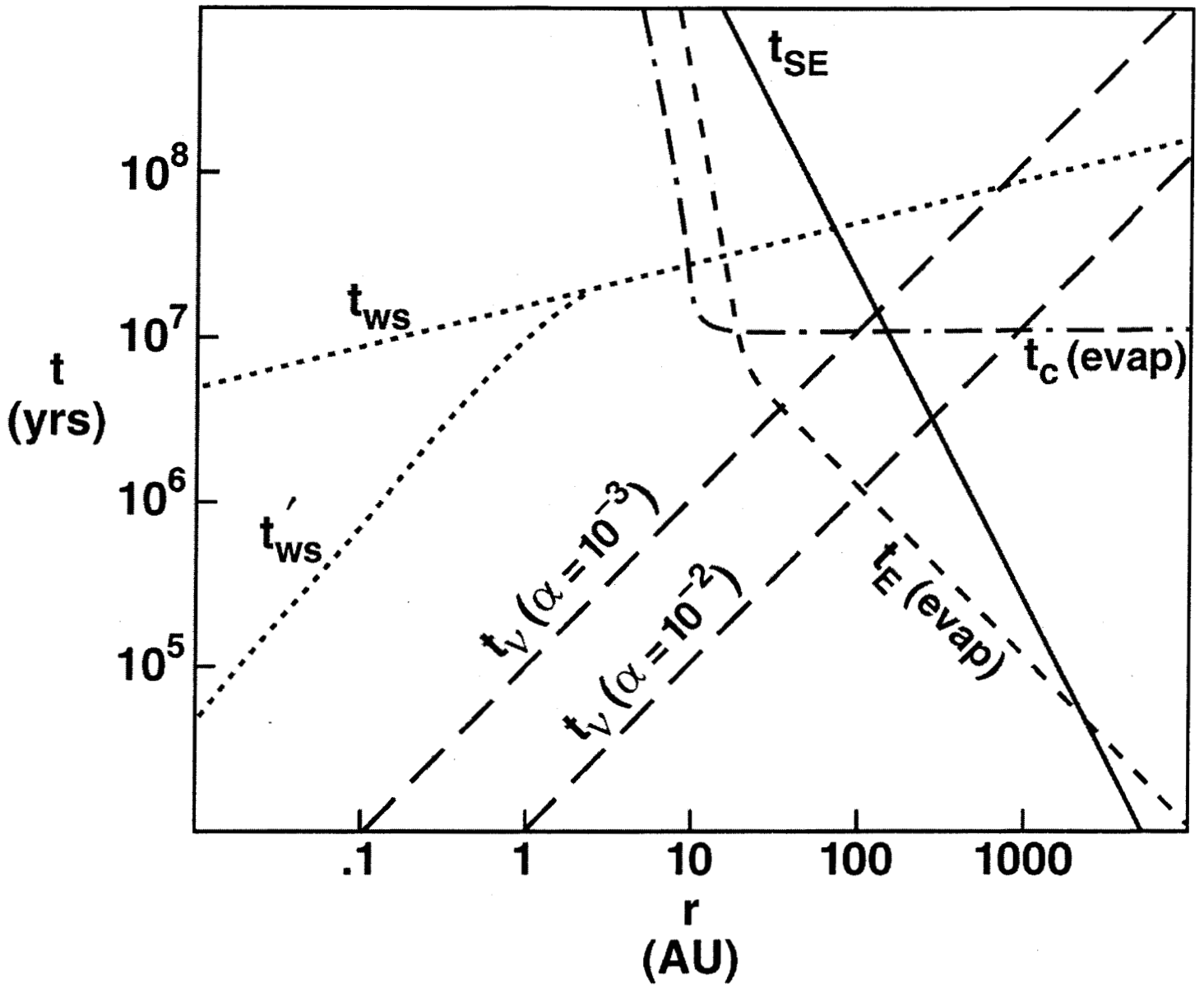


Fig. 2

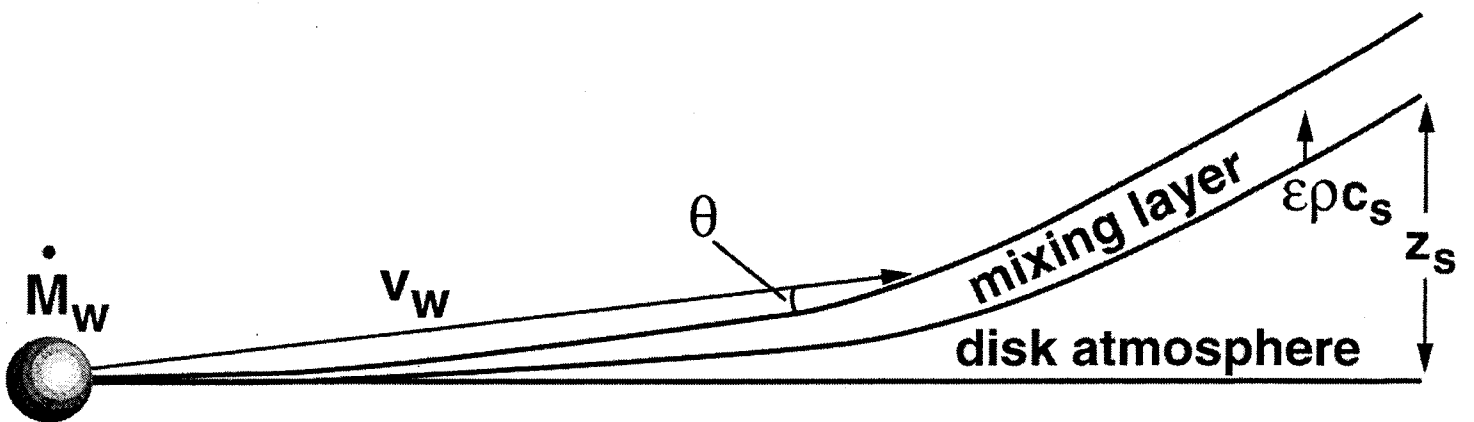
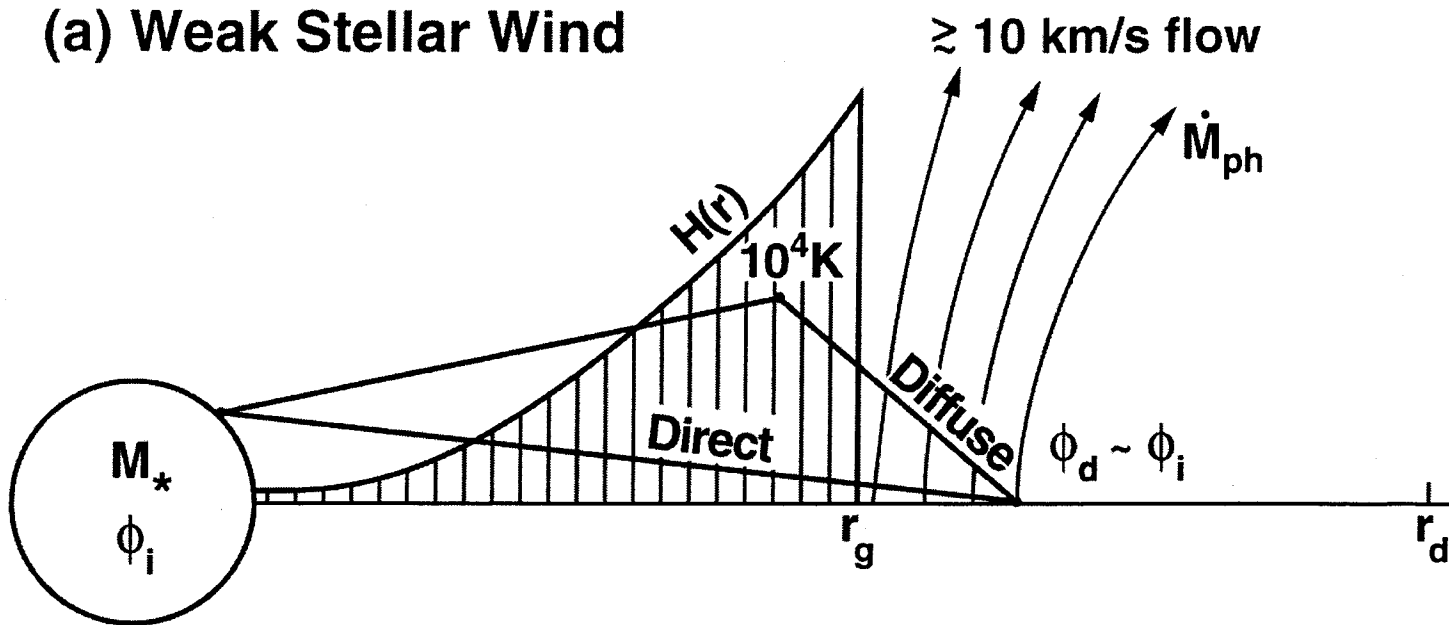


Fig. 3

(a) Weak Stellar Wind



(b) Strong Stellar Wind

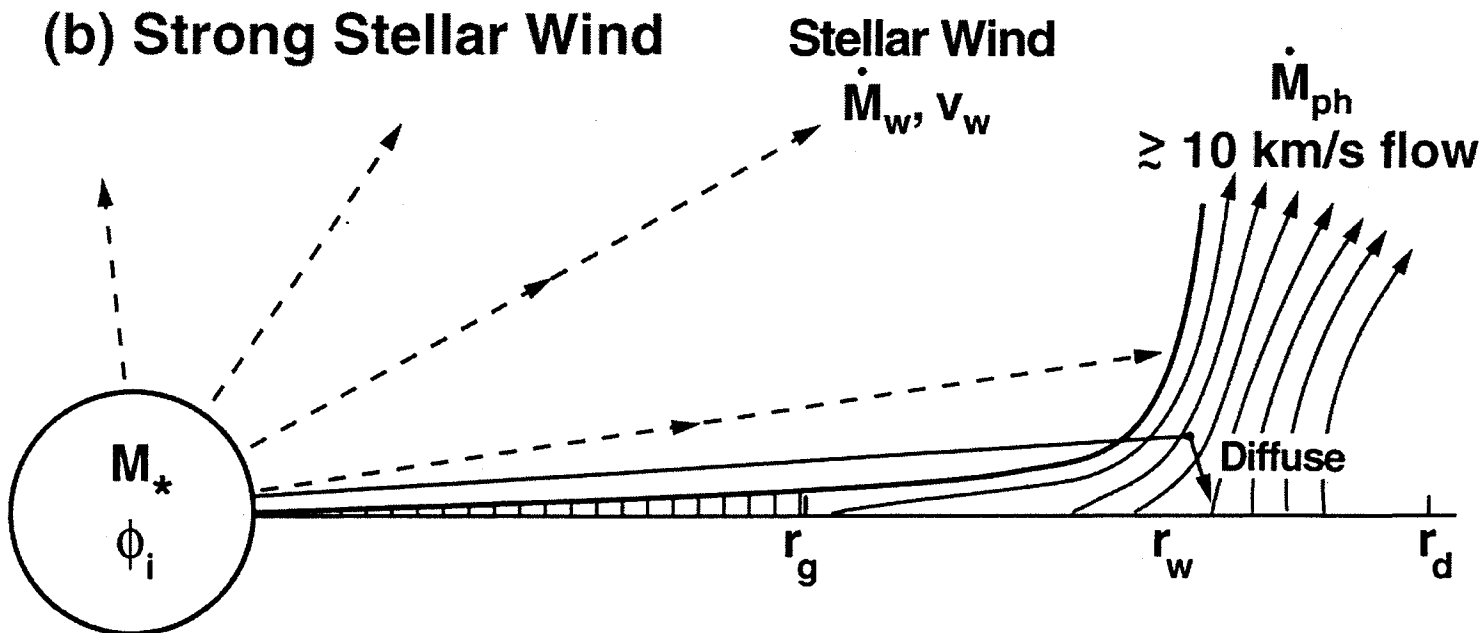


Fig. 4

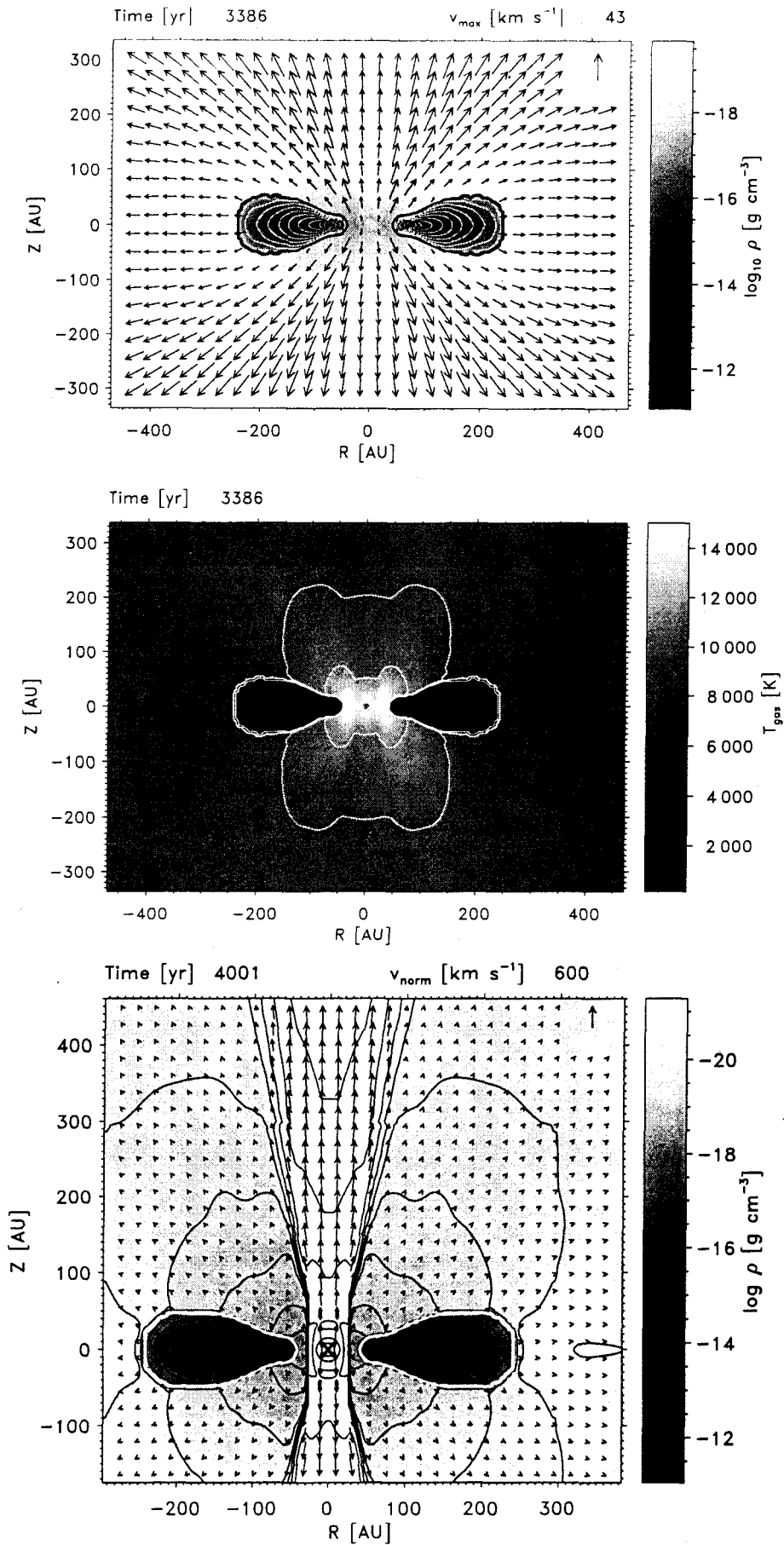


Fig. 5

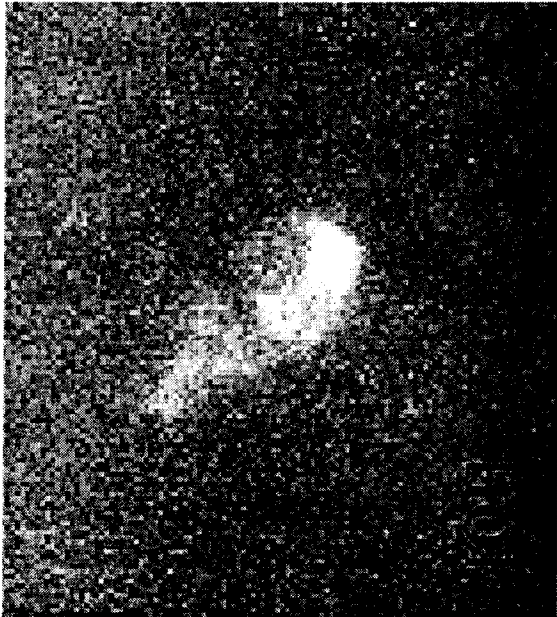


Fig. 6

